RESEARCH PAPER

PCCP
www.rsc.org/pccp

Rovibrational analysis of the absorption spectrum of HDO between 10 110 and 12 215 cm^{-1} †

O. Naumenko,[ab] S.-M. Hu,[c] S.-G. He[c] and A. Campargue[a]

[a] *Laboratoire de Spectrométrie Physique (associated with CNRS, UMR 5588), Université Joseph Fourier de Grenoble, B.P. 87, 38402 Saint-Martin-d'Hères Cedex, France*
[b] *Institute of Atmospheric Optics, Russian Academy of Science, Tomsk, Russia*
[c] *Laboratory of Bond-Selective Chemistry, University of Science and Technology of China, Hefei 230026, China*

Received 9th October 2003, Accepted 19th December 2003
First published as an Advance Article on the web 2nd February 2004

The weak absorption spectrum of monodeuterated water has been investigated between 10 110 and 12 215 cm^{-1} by high resolution Fourier transform absorption spectroscopy with a 105 m absorption pathlength. The spectrum is dominated by the $4\nu_1$, $3\nu_3$, and $\nu_2+3\nu_3$ bands at 10 378.95, 10 631.68 and 11 969.76 cm^{-1}, respectively. The rovibrational assignment was performed on the basis of the *ab initio* calculations of Schwenke and Partridge and by using the effective Hamiltonian approach. 502 energy levels belonging to a total of 13 vibrational states were determined. The rotational structure of the (003) state is mostly isolated and could be fitted with an rms of 0.006 cm^{-1}, slightly larger than the experimental uncertainty. Most of the other levels are connected *via* a complex interaction scheme involving dark states which prevented a satisfactory modeling. The analysis of the rotational structure of the (013), (400) and (112) states is investigated for the first time, while the existing information for the (003) state is considerably enlarged and improved. Transitions reaching the nine other (dark) states, including the highly excited bending states, (051), (061) and (080), were detected in the spectrum as a result of intensity borrowing due to resonance interactions with bright states.

I. Introduction

The knowledge of the rovibrational energy levels of monodeuterated water is much less complete than that of the main isotopomer, $H_2{}^{16}O$, particularly in terms of line intensities. However, numerous new experimental data have been obtained on the rotational structure of the HDO vibrational states both by high resolution Fourier transform (FT) absorption spectroscopy[1–6] and intracavity laser absorption spectroscopy (ICLAS).[7–14] In addition, great progress has been recently achieved in the calculation of water vapor absorption spectra from high quality *ab initio* potential and dipole moment surfaces.[15,16]

The present contribution is devoted to the analysis of the HDO absorption spectrum investigated between 10 110 and 12 215 cm^{-1} by Fourier transform absorption spectroscopy with a 105 m absorption pathlength (see Fig. 1). The 9625–10 100 cm^{-1} region, which is just below the region of interest, was very recently analyzed by ICLAS based on vertical external cavity surface emitting lasers (VeCSEL).[13] The high sensitivity of ICLAS, allowed a significant improvement over a previous study performed in that region on the basis of the same FT spectrum presently investigated.[5]

As labeled in Fig. 1, the absorption spectrum of HDO in the considered region, is dominated by the $4\nu_1$, $3\nu_3$ and $\nu_2+3\nu_3$ bands at 10 378.95, 10 631.68 and 11 969.76 cm^{-1} respectively (we use the traditional labeling of the vibrational modes: ν_1(2723.68 cm^{-1}), ν_2(1403.48 cm^{-1}) and ν_3(3707.47 cm^{-1}) for the OD stretching, the bending and the OH stretching vibration, respectively). The $3\nu_3$ band was previously investigated between 10 280 and 10 770 cm^{-1} by ICLAS based on a $F_2{}^+$:LiF color center laser.[14] The analysis of the spectrum (317 lines) resulted in the derivation and modeling (rms = 0.028 cm^{-1}) of 97 observed energy levels of the (003) state. However, the quality of the FT spectrum presently analyzed allowed us to improve this analysis both in term of sensitivity and in term of accuracy. For completeness, we should mention the analysis of the low JK_aK_c levels of the (003) state

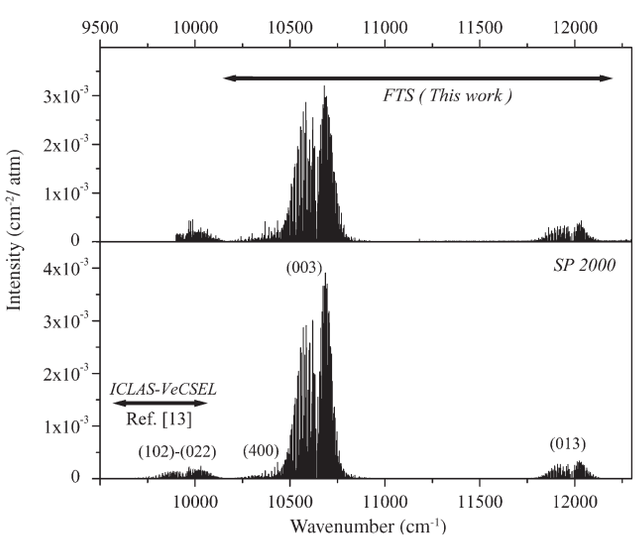

Fig. 1 Overview of the HDO spectrum between 9500 and 12 500 cm^{-1}. Upper panel: stick spectrum retrieved from the FT spectrum recorded with a 105 m absorption pathlength at a total pressure of water of 15 hPa. Lower panel: stick spectrum calculated by Schwenke and Partridge (SP 2000) from *ab initio* potential energy and dipole moment surfaces.[16] The normal mode labeling of the upper vibrational state of the dominant transitions is given.

† Electronic supplementary information (ESI) available: HDO absorption spectrum and rotational assignments. See http://www.rsc.org/suppdata/cp/b3/b312514a/

DOI: 10.1039/b312514a

observed by photoacoustic spectroscopy using an injection seeded optical parametric oscillator (OPO)[17] which allowed the transition moment alignment in HOD to be studied.[18] To the best of our knowledge, the analysis of the $4\nu_1$ and $\nu_2+3\nu_3$ bands has not been previously reported.

II. Experimental details

The sample of D_2O was purchased from Peking Chemical Industry, Ltd (China). The stated deuterium purity is 99.8%. The spectra obtained in Hefei (China) were recorded at room temperature with a Bruker IFS 120 HR Fourier Transform interferometer equipped with a pathlength adjustable multipass cell, a tungsten light source, a CaF_2 beam splitter, and a Si-diode detector. The unapodized resolution was 0.02 cm^{-1} and the absorption pathlength was 105 m. Since in the region under study many lines are due to D_2O and H_2O, two samples were prepared in order to discriminate the different isotopomers from the relative line intensities, as illustrated in Fig. 2. The first one was a 1:1 mixture of H_2O and D_2O at a pressure of 15 hPa which is assumed to lead to a mixture of H_2O:HDO:D_2O in the proportion 1:2:1. In the second one, the D_2O concentration was much higher. The FT spectrum was calibrated with water lines listed in the HITRAN database. The accuracy of the absolute positions of unblended lines is estimated to be around 0.002 cm^{-1}.

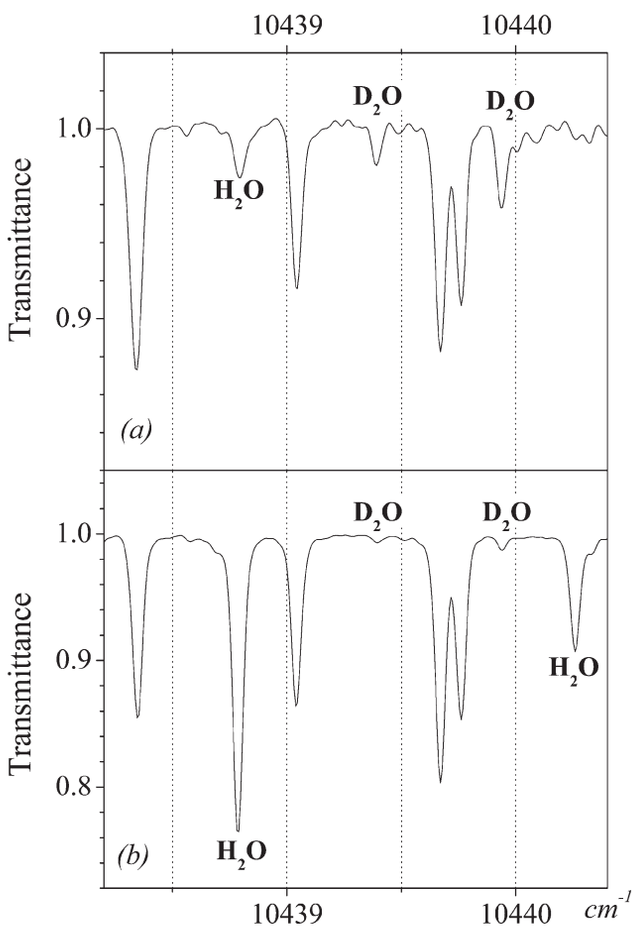

Fig. 2 Comparison of a section of the FT spectra obtained with different proportion of water isotopomers ($P = 15$ hPa, $l = 105$ m). The lower panel (*b*) corresponds to a mixture of H_2O:HDO:D_2O in the proportion 1:2:1 while the upper panel (*a*) was recorded with a large amount of deuterated water. The variation of the relative intensities helps to discriminate the HDO lines: compared to HDO lines, the H_2O lines are much stronger in (*b*) than in (*a*) while it is the opposite for D_2O lines. The lines due to D_2O and H_2O are indicated.

III. Spectrum assignment and energy level determination

Our recent high sensitivity ICLAS investigation covered the 9625–10 100 cm^{-1} region.[13] We thus limit the present analysis of the FT spectrum to the region just above 10 100 cm^{-1}. About 1800 absorption lines, observed between 10 110 and 12 215 cm^{-1}, were attributed to HDO, some of them being blended by H_2O and D_2O lines. For identification purposes, approximate intensities were derived for all observed lines from their peak absorption. The spectral assignment was performed relying on the Schwenke and Partridge (SP) database,[15,16] which predicts accurate line positions and intensities for H_2O and its isotopomers. A computer code developed for automatic rovibrational spectrum assignment was also intensively exploited.[19] This program used the SP synthetic spectrum and experimental line positions and intensities as input data. Of all HDO lines, 1579 were rovibrationally assigned which, taking into account the unresolved multiplets, corresponds to 1827 transitions reaching 13 upper vibrational states.

The experimental information obtained is summarized in Table 1 while the resulting line list, which includes the experimental line positions and SP calculated intensities followed by the rovibrational assignment, is available as electronic supplementary information (ESI).† Note that, as shown in Fig. 1, the analyzed spectral region consists in two well isolated parts, 10 110–11 452 cm^{-1} and 11 750–12 215 cm^{-1}, corresponding mainly to the $3\nu_3$ and $\nu_2+3\nu_3$ bands, respectively. In the region in between, the HDO absorption lines were too weak to be reliably identified.

Accurate upper energy levels for all observed transitions were derived by adding the ground state rotational term values.[20] The total number of energy levels obtained for every observed vibrational state is presented in Table 1 while their values are listed in Tables 2 and 3, which also include their experimental uncertainty and the deviations from SP predictions. In order to check and confirm SP rovibrational assignment, we attempted to reproduce the observed energy levels with the effective Hamiltonian (EH) approach (see next section). However, in most cases we did not succeed in performing a complete EH fitting due to the lack of sufficient experimental information since the three analyzed "bright" states, (400), (013) and (112), were strongly perturbed by many "dark" states (see next Section). However, the EH modeling, though being not fully satisfactory, allowed the correction of some SP assignments and added to the understanding of the resonance scheme involved in the considered polyads of interacting states. The only successful fit was achieved for the (003) state, which appears to be mostly isolated from the other vibrational states.

Tables 2 and 3 show that the deviations of SP prediction from the observed energy levels can reach a value of 0.43 cm^{-1} for some vibrational states. However, as we have already stressed,[13] these deviations vary regularly with J and K_a. This feature combined with a reasonable agreement between calculated[16] and experimental intensity values and supported by the systematic use of the ground state combination difference (GSCD) method, provided a complete and reliable assignment of the observed spectrum. Fig. 1 and Fig. 3 show the overall excellent agreement between the observed and calculated[16] spectrum in the whole region and an expanded section, respectively. As a result, 502 energy levels were derived and assigned to 13 vibrational states. The only previous reports relevant to these states are (*i*) an ICLAS study of the (003) state near 10 500 cm^{-1}, which led to the derivation of 97 energy levels;[14] (*ii*) the photoacoustic spectroscopy of the same (003) state from which 13 low JK_aK_c levels were derived,[17] and (*iii*) our ICLAS-VeCSEL study in the 9625–10 100 cm^{-1} region[13] which allowed us to determine 35 and 11 energy levels from hot bands transitions, for the (032) and (112) states, respectively.

Table 1 Summary of the HDO experimental information obtained in the 10 110–12 215 cm^{-1} spectral region

E_v/cm^{-1}					
SP[15,16]	Observed	$v_1v_2v_3$	Integrated intensity[a] /$cm^{-2}atm^{-1}$	Number of transitions	Number of levels
10 119.37		(080)	3.45×10^{-5}	7	2
10 318.55		(051)	2.21×10^{-4}	25	12
10 378.64	10 378.9511	(400)	3.58×10^{-3}	231	89
10 403.21	10 403.1422	(211)	1.55×10^{-4}	34	19
10 480.73		(131)	1.40×10^{-4}	8	2
10 631.92	10 631.6832	(003)	2.78×10^{-1}	983	172
10 652.52		(320)	1.00×10^{-3}	20	9
11 243.06	11 242.923	(032)	4.75×10^{-6}	4	4
11 315.43	11 315.4333	(112)	3.83×10^{-4}	81	53
11 533.48		(061)[b]	4.90×10^{-6}	3	1
11 804.57		(141)	4.50×10^{-5}	10	7
11 958.26		(330)[b]	4.65×10^{-4}	17	9
11 970.07	11 969.7584	(013)	1.90×10^{-2}	320	123

[a] The integrated intensities were obtained from the sum of the calculated[16] pure HDO intensities of all assigned transitions for a given vibrational band. [b] Integrated intensities for the (061)–(000) and (330)–(000) bands seem to be distorted (see text).

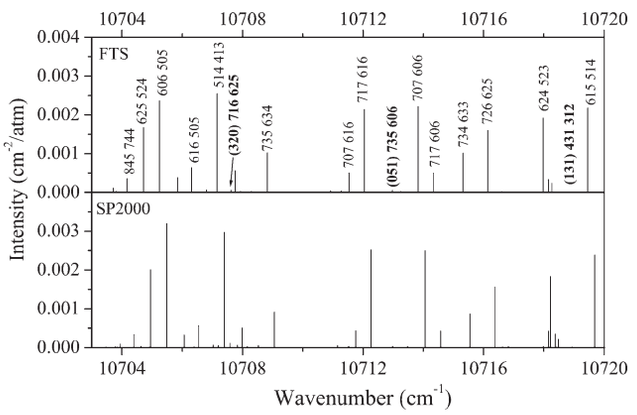

Fig. 3 The FT absorption spectrum of HDO in the 10 703–10 720 cm^{-1} spectral region corresponding to a section of the $3\nu_3$ band centered at 10 631.683 cm^{-1}. The $J'K'_aK'_c$–$J''K''_aK''_c$ rotational assignments are given for some of the lines (all of the assignments are listed in the ESI†). The rotational assignments written in bold characters are those of extra lines borrowing their intensities from transitions of the $3\nu_3$ band (see text). The upper panel is a stick spectrum retrieved from the FT spectrum recorded with a 105 m absorption pathlength at a total pressure of water of 15 hPa. The lower panel is the HDO spectrum calculated by Schwenke and Partridge from *ab initio* potential energy and dipole moment surfaces.[16]

For completeness, we include in Table 3 the energy levels of the (032) state obtained by ICLAS-VeCSEL.[13] Compared to the extensive set of levels obtained for the (102)–(022) interacting dyad,[13] five additional levels, listed in Table 3, could be determined. It is worth noticing that in accordance with the wave function mixing obtained in the fitting of the (112)–(032) dyad, we inverted some vibrational assignments of the (032) and (112) states with respect to those in ref. 13. The values of ref. 14 for the energy levels of the (003) state show deviations of 0.07 cm^{-1} on average from our more precise values, with a maximum discrepancy of 0.14 cm^{-1}. Five energy levels were incorrect. Thus, the total number of newly derived energy levels is 404, while the determination of the 92 previously determined energy levels of the (003) state is significantly improved.

IV. Effective Hamiltonian and resonance interactions with dark states

Numerous strong resonance interactions between the analyzed vibrational states were evidenced during the spectral assignment and modeling process. In many cases, these interactions induce important intensity transfer to weak transitions, which would have been unobservable in absence of such couplings.

The (003) state belongs to the sequence of the $(00v_3)$ states corresponding to the excitation of the OH stretch, which is expected to be isolated from the other vibrational states. The (004),[7] (005),[10] (006) and (007)[4,21] states could also be considered as well isolated. Note, however, that the observation of some line-resonance partners from dark upper states has revealed noticeable perturbations affecting both the (004) and the (005) states. The (003) state with a band origin at 10 631.6832 cm^{-1} can also be treated as a nearly isolated state. We could reproduce 160 of the 172 observed energy levels with a rms deviation of 0.006 cm^{-1} by using an effective rotational Hamiltonian written using Padé–Borel approximants[22,23] and by adjusting 16 parameters. These parameters are listed in Table 4, while the (obs. − calc.) values of the energy levels are given in Table 2. The comparison included in Table 4 with the parameters previously obtained show a very good agreement (except for the vibrational term) with ref. 14, but significant differences with ref. 17. This disagreement can be explained by the fact that only 13 low $[JK_aK_c]$ energy levels were obtained and included in the fit of ref. 17 and by the fact that three of these levels, [313], [532] and [524], were found to have errors as large as 1.07 cm^{-1}.

Overall 13 energy levels of dark states were derived through transitions borrowing their intensities *via* resonance interaction with the rotational levels of the bright (003) state. They belong to the following vibrational states: (320) (9 levels), (131) (2 levels), (051) (1 level), and (080) (1 level) (see Table 3). Interestingly the (003) energy level shifts, caused by all these resonance interactions, are very small: all the interacting energy levels could indeed be included in the EH fit, except the (003) [716] level at 11 092.0415 cm^{-1} which deviates from its unperturbed position by −0.068 cm^{-1} due to interaction with the (320) [716] level at 11 092.5192 cm^{-1}, observed through five lines. Indeed, this interaction induces a strong intensity transfer (up to 50%!) to the extra lines of the (320) upper state.

In contrast to the (003) state, the pure OD stretching (400) state at 10 378.9511 cm^{-1} was found to be strongly perturbed and could not be fitted as an isolated state. Already at $J = 2$, all energy levels with $K_a = 2$ interact strongly with the corresponding $K_a = 2$ levels of the (051) state. As J increases, the energy levels with $K_a = 1$ gradually become involved in the resonance. This interaction results in the observation of eleven energy levels of the (051) state. A further

Table 2 Rotational energy levels (in cm^{-1}) of the (003), (013), (400), and (112) vibrational states of HDO[a]

	(003)					(013)				(400)				(112)			
JK_aK_c	E_{obs}/cm^{-1}	σ	N	δ	Δ	E_{obs}/cm^{-1}	σ	N	Δ	E_{obs}/cm^{-1}	σ	N	Δ	E_{obs}/cm^{-1}	σ	N	Δ
0 0 0	10 631.6832	0.5	2	−5	−23	11 969.7584		1	−30	10 378.9511		1	31	11 315.4333		1	0
1 0 1	10 646.9209	0.7	4	−5	−23	11 985.0655	0.2	2	−30	10 393.4742	2.5	2	31	11 330.6251	3.5	2	−1
1 1 1	10 658.2329	0.2	4	1	−23	11 997.7239	0.3	2	−29	10 408.2096	0.3	2	29	11 345.1810		1	−2
1 1 0	10 661.1253	0.2	3	2	−23	12 000.8530	0.2	2	−29	10 410.7151	1.4	3	30	11 348.2613		1	−1
2 0 2	10 676.9016	0.5	4	−5	−24	12 015.1657	0.4	2	−30	10 422.1939	0.4	2	31	11 360.5839 I	4.0	2	−2
2 1 2	10 685.8082	0.3	5	0	−23	12 025.1671	0.1	2	−24	10 434.6930		1	29	11 372.5745 I	2.7	2	−3
2 1 1	10 694.4782	0.3	6	3	−23	12 034.5587	0.3	3	−27	10 442.1948	0.7	2	29	11 381.7429	11.1	2	−2
2 2 1	10 728.2769	0.2	4	0	−22	12 072.6148	0.3	2	−30	10 486.5708		1	13	11 425.9575	6.0	2	−1
2 2 0	10 728.7625	0.4	4	0	−22	12 073.1203	0.4	2	−29	10 486.8462	0.5	3	14	11 426.3931 I		1	−1
3 0 3	10 720.7236	0.9	4	−7	−24	12 059.1114	0.7	3	−31	10 464.5207	0.4	3	31	11 404.4839	0.4	2	−3
3 1 3	10 726.8779	0.6	7	0	−23	12 066.4296	0.3	2	−19	10 474.2346	0.2	3	29	11 413.0864	1.2	2	−5
3 1 2	10 744.1453	0.2	5	4	−23	12 084.6845	0.4	2	−14	10 489.1680	1.0	3	29	11 431.6699	0.6	2	−2
3 2 2	10 773.9442	0.2	6	5	−23	12 118.4943	0.3	3	−30	10 530.8539	0.7	2	7	11 471.6485 I	7.8	2	−2
3 2 1	10 776.2778	0.3	7	2	−23	12 120.9352	0.8	3	−30	10 532.2193	0.7	2	8	11 473.7583	9.1	2	0
3 3 1	10 837.3960	0.5	4	4	−21	12 189.2570	0.2	2	−27	10 602.5402	0.3	3	22	11 555.6234	7.6	2	−2
3 3 0	10 837.4472	1.1	6	4	−21	12 189.3079	0.0	2	−28	10 602.5574	2.2	2	22	11 555.6035		1	−4
4 0 4	10 777.4061	0.6	6	−4	−23	12 115.8496	0.5	2	−30	10 519.7165	0.2	2	30	11 461.3680	1.8	2	−2
4 1 4	10 781.1586	0.3	6	−1	−23	12 120.2967	0.2	2	−20	10 526.6379	2.2	3	30	11 467.2098	0.7	2	−2
4 1 3	10 809.6231	0.4	5	6	−24	12 151.2261	0.3	2	−22	10 551.4045	0.4	4	27	11 497.6150	1.5	2	−2
4 2 3	10 834.3934	0.3	7	−15	−23	12 179.2353	0.4	3	−30	10 581.2398	1.0	2	17	11 532.2232 I	4.8	2	−2
4 2 2	10 840.9191	0.5	7	2	−23	12 186.0546	0.3	3	−30	10 585.7546	1.0	2	20	11 538.1657		1	−2
4 3 2	10 899.0329	0.4	6	4	−22	12 251.2185	0.5	3	−28	10 660.5294	0.3	2	23	11 617.6196	3.3	2	0
4 3 1	10 899.3878	0.4	7	4	−21	12 251.5744	0.3	2	−27	10 660.6731	1.0	2	22	11 617.8379	3.6	2	0
4 4 1	10 985.9618	3.0	5	−6	−22	12 347.9676	4.4	2	−25	10 764.6908	6.0	2	16	11 739.5909 I		1	−2
4 4 0	10 985.9630	2.4	4	−10	−22	12 347.9748	4.6	2	−25	10 764.6814	1.5	2	16	11 739.5890 I		1	−2
5 0 5	10 846.2961	0.5	7	−4	−24	12 184.6684	0.5	2	−31	10 587.1330	0.4	2	30	11 530.4815	2.5	2	−2
5 1 5	10 848.3666	0.4	7	−1	−24	12 187.1611	0.0	2	−30	10 591.7025	2.2	3	29	11 534.0419 I	9.6	2	−3
5 1 4	10 890.1461	0.5	8	9	−25	12 232.4550	1.0	4	−29	10 628.9840	1.4	3	23	11 578.9381		1	−3
5 2 4	10 909.3412	0.5	7	−4	−23	12 254.4885	1.2	3	−30	10 654.0890	0.9	2	26	11 607.3936 I	3.4	2	−2
5 2 3	10 922.9291	0.3	8	2	−24	12 268.7728	0.2	2	−31	10 663.2086	0.8	3	27	11 620.0915		1	−2
5 3 3	10 976.1700	0.4	7	4	−22	12 328.7706	0.8	4	−29	10 733.0702	0.0	2	23	11 695.2210		1	0
5 3 2	10 977.5350	0.6	4	4	−22	12 330.1801	0.4	2	−26	10 733.6328	0.3	2	23				
5 4 2	11 062.9136	1.1	5	−1	−19	12 425.3531	2.0	2	−26	10 836.8307		1	18				
5 4 1	11 062.9532	0.4	3	−2	−20	12 425.3868		1	−25	10 836.8272	2.0	2	16				
5 5 1	11 173.4008	1.0	3	2	−18	12 547.4231	0.0	2	−24	10 968.9128		1	8	11 977.2863		1	−2
5 5 0	11 173.4006	0.3	3	1	−18	12 547.4237	0.6	2	−24	10 968.9128		1	8	11 977.2863		1	−2
6 0 6	10 927.1946	0.5	7	−5	−25	12 265.3143	0.3	2	−30	10 666.3889	0.3	2	30	11 611.4589		1	−2
6 1 6	10 928.2572	0.5	8	−4	−24	12 266.6226		1	−31	10 669.2193	1.1	2	29	11 613.4937	3.0	2	−3
6 1 5	10 984.6911	0.5	8	19	−25	12 327.8755	1.3	2	−30	10 715.8139	1.8	2	28	11 674.7787		1	−2
6 2 5	10 998.3525	0.7	4	−3	−24	12 343.8619	0.4	2	−30	10 739.7832	3.1	3	28	11 696.8059	1.5	2	−2
6 2 4	11 021.9768	0.7	6	1	−25	12 368.7801	0.2	2	−31	10 755.9417	1.0	2	29	11 719.4132	4.9	2	−3
6 3 4	11 068.6870	0.4	6	3	−23	12 421.7972	2.1	3	−29	10 820.1242	0.1	2	23	11 788.4278		1	1
6 3 3	11 072.5208	0.3	7	3	−23	12 425.6718	1.1	3	−30	10 821.7540	0.6	2	23	11 791.1673		1	−2
6 4 3	11 155.4660	0.8	6	−1	−21	12 518.4365	0.7	2	−24	10 923.4723		1	20				
6 4 2	11 155.6626	0.6	5	0	−21	12 518.6461	0.7	3	−24	10 923.5267	3.8	2	16				
6 5 2	11 265.4731	1.2	6	1	−19	12 639.9821	2.4	3	−24	11 055.0393		1	8				
6 5 1	11 265.4734	1.1	4	−3	−19	12 639.9840	2.3	3	−25	11 055.0462		1	9				
6 6 1	11 398.7914	0.4	4	1	−16	12 786.6845		1	−21	11 214.5218	0.6	2	0				
6 6 0	11 398.7912	0.3	3	1	−16	12 786.6846		1	−21	11 214.5218	0.6	2	0				
7 0 7	11 020.1461	0.3	4	7	−24	12 357.8145	1.1	2	−32	10 757.3682	1.0	3	29	11 704.2390		1	−3
7 1 7	11 020.6581	0.5	6	0	−23	12 358.4684	1.7	2	−31	10 759.0413	1.4	3	28	11 705.3647		1	−3
7 1 6	*11 092.0415	0.6	6	−68	−43	12 436.3499	0.9	2	−24	10 820.8888	0.7	3	31	11 784.1163		1	−2
7 2 6	11 101.0149	0.5	7	−2	−24	12 446.7815	0.8	2	−31	10 838.7283	0.5	2	23	11 800.1176 I		1	−1
7 2 5	11 137.3365	0.6	5	−1	−25	12 485.3411	1.2	2	−33	10 864.0910		1	30	11 835.5169		1	−2
7 3 5	11 176.3410	0.4	5	3	−24	12 530.0501	1.4	3	−30	10 921.6150	1.0	2	23				
7 3 4	11 184.9815	0.7	7	1	−24	12 538.8208	0.6	3	−31	10 925.4328		1	24				
7 4 4	11 263.6688	0.6	5	0	−22	12 627.2236		1	−27	11 024.7070	0.9	3	17				
7 4 3	11 264.3604	0.7	5	0	−22	12 628.0762	2.0	3	−25	11 024.8982	2.2	2	17				
7 5 3	11 373.0665	1.7	3	−3	−20	12 748.1354		1	−23	11 155.5794		1	7				
7 5 2	11 373.0913	1.7	3	−2	−20	12 748.1652		1	−25	11 155.6092		1	9				
7 6 2	11 505.8706	0.8	3	2	−16	12 894.3257		1	−22	11 314.4874		1	0				
7 6 1	11 505.8694	1.8	4	0	−16	12 894.3257		1	−22	11 314.4874		1	0				
7 7 1	11 661.1358	0.7	5	−1	−12	13 064.2464		1	−17	11 500.6005		1	−7				
7 7 0	11 661.1358	0.7	5	−1	−12	13 064.2464		1	−17	11 500.6005		1	−7				
8 0 8	11 125.1840	0.4	5	−3	−26	12 462.2466		1	−31	10 860.0753	0.5	2	28	11 808.8864		1	−5
8 1 8	11 125.4317	0.2	4	−1	−25	12 462.5663	2.9	2	−31	10 861.1082	0.7	2	27	11 809.5033		1	−4
8 1 7	11 211.5757	0.6	6	−13	−25	12 556.4570		1	−31	10 937.7609	0.0	2	30	11 905.9933		1	−4

Table 2 (continued)

	(003)					(013)				(400)				(112)			
JK_aK_c	E_{obs}/cm^{-1}	σ	N	δ	Δ	E_{obs}/cm^{-1}	σ	N	Δ	E_{obs}/cm^{-1}	σ	N	Δ	E_{obs}/cm^{-1}	σ	N	Δ
8 2 7	11 216.9224	0.7	7	0	−25	12 563.0174	1.6	2	−30	10 950.1189	1.5	2	28	11 916.9268		1	−1
8 2 6	11 268.0330	0.9	8	−3	−27	12 617.4500	0.6	2	−33	10 987.3605		1	31				
8 3 6	11 298.7778	0.4	6	4	−24	12 653.1799	0.7	2	−31	11 037.2592	3.6	2	23	12 020.7880		1	−2
8 3 5	11 315.2098	0.5	7	−2	−26	12 669.9637	0.4	2	−32	11 045.1047		1	26	12 033.8027		1	−2
8 4 5	11 387.5001	0.8	6	2	−23	12 751.5967	1.6	2	−28	11 140.5197	0.8	2	18				
8 4 4	11 389.4571	0.5	6	0	−23	12 753.2785	3.6	2	−30	11 141.0908		1	19				
8 5 4	11 496.2545	0.9	5	−4	−19	12 871.9621	2.6	2	−28	11 270.6271		1	11				
8 5 3	11 496.3511	0.9	7	−4	−21	12 872.0654	0.8	2	−27	11 270.6340		1	11				
8 6 3	11 628.3688	0.5	3	4	−17	13 017.4798		1	−21								
8 6 2	11 628.3695	0.9	3	3	−18	13 017.4793		1	−22								
8 7 2	11 783.0785	1.5	3	−4	−14	13 186.8068		1	−21								
8 7 1	11 783.0788	1.4	4	−4	−14	13 186.8068		1	−21								
8 8 1	11 959.3797	0.7	2	3	−10												
8 8 0	11 959.3797	0.7	2	3	−10												
9 0 9	11 242.3879	0.3	5	1	−26	12 578.6638		1	−33	10 974.4522	0.4	2	28	11 925.4476		1	−7
9 1 9	11 242.5058	0.6	5	5	−26	12 578.8147		1	−33	10 975.6009	0.5	2	25				
9 1 8	11 342.7240	0.9	5	−6	−26	12 688.3185	3.7	2	−30	11 064.2217		1	34				
9 2 8	11 345.7137	0.4	5	−1	−26	12 692.0701	0.2	2	−31								
9 2 7	11 412.9010	0.1	4	−4	−27	12 763.9101		1	−34	11 125.2122		1	33	12 046.8614		1	−2
9 3 7	11 435.5609	0.3	6	3	−26	12 790.8031	3.0	2	−27	11 166.7731		1	25				
9 3 6	11 462.9235	0.9	6	−1	−27	12 818.8776	2.7	2	−33	11 181.0421	0.0	2	28				
9 4 6	11 526.8300	0.9	5	2	−24	12 891.6368		1	−30								
9 4 5	11 531.5089	1.0	8	−2	−25	12 896.0611		1	−30	11 272.3191		1	20				
9 5 5	*11 635.0565	1.4	2	−36	−21	13 011.5216		1	−29								
9 5 4	*11 635.3744	1.0	3	−42	−21	13 011.8229	6.7	2	−29								
9 6 4	11 766.3313	1.2	3	8	−19	13 156.1551		1	−23								
9 6 3	11 766.3395	3.8	2	5	−20	13 156.1556		1	−25								
9 7 3	11 920.3366	2.2	5	−1	−15	13 324.7837		1	−22								
9 7 2	11 920.3371	2.7	5	−1	−15	13 324.7836		1	−22								
9 8 2	12 096.0241	0.3	2	−5	−12												
9 8 1	12 096.0241	0.3	2	−5	−12												
10 0 10	11 371.7562	1.3	5	2	−26	12 707.0907		1	−34	11 100.5294	1.2	2	27				
10 1 10	11 371.8055	1.7	2	0	−26	12 707.1610		1	−34								
10 1 9	11 485.5208	0.9	4	4	−26	12 831.6381	0.9	2	−32	11 205.7091		1	30				
10 2 9	11 487.1040	1.5	3	−2	−27	12 833.6803	1.8	2	−33	11 211.1364		1	30				
10 2 8	11 570.7061	1.1	4	−2	−27	12 923.4168	0.0	2	−35	11 276.8914		1	33				
10 3 8	11 586.2178	0.7	6	4	−26	12 942.1895		1	−33	11 310.3053		1	27				
10 3 7	11 627.3294	1.0	3	−1	−28	12 984.7770		1	−35								
10 4 7	11 681.4159	0.9	3	2	−25	13 047.1120		1	−34								
10 4 6	11 691.1102	0.8	4	−4	−27	13 056.8321		1	−31								
10 5 6	11 789.5943	0.5	5	8	−24	13 166.8001		1	−32								
10 5 5	11 790.5113	1.2	3	7	−23												
10 6 5	11 919.7816	2.3	3	−7	−20												
10 6 4	11 919.8202	2.0	3	−12	−20												
10 7 4	12 072.9418	0.3	3	18	−17												
10 7 3	12 072.9401	1.6	4	15	−17												
11 0 11	11 513.2824		1	3	−27	12 847.5269		1	−34	11 238.4974		1	27				
11 1 11	11 513.2931	6.0	2	−10	−30	12 847.5714		1	−34	11 235.0284		1	25				
11 1 10	11 640.0636	0.5	4	−3	−27	12 986.5127		1	−34								
11 2 10	11 640.8845	1.9	3	1	−27	12 987.5898		1	−34								
11 2 9	11 740.4016	0.4	3	−2	−29	13 094.8466		1	−35								
11 3 9	11 750.2738	2.1	4	3	−28	13 107.1285		1	−32								
11 3 8	11 807.3350	1.9	4	−2	−29	13 166.5269		1	−27								
11 4 8	11 850.8996	0.6	3	3	−26	13 217.5995		1	−35								
11 4 7	11 868.6056	0.8	4	−7	−28	13 235.1242		1	−37								
11 5 7	11 959.6803	0.7	3	−11	−25												
11 5 6	11 961.9495	0.6	2	−18	−25												
11 6 6	12 088.8061	7.3	2	7	−20												
11 6 5	12 088.9240	2.9	2	−18	−22												
11 7 5	*12 240.9120		1	47	−18												
11 7 4	*12 240.9017		1	31	−18												
11 8 4	12 414.9341		1	−2	−14												
11 8 3	12 414.9339		1	−2	−14												
12 0 12	11 666.9441	3.3	2	2	−29	12 999.9345		1	−37								
12 1 12	11 666.9605	4.2	2	8	−28	12 999.9622		1	−36								
12 1 11	11 806.4885	0.3	5	1	−28	13 153.1689		1	−33								
12 2 11	11 806.9018	0.4	2	5	−28	13 153.7202		1	−35								

Table 2 (continued)

	(003)					(013)				(400)				(112)			
JK_aK_c	E_{obs}/cm^{-1}	σ	N	δ	Δ	E_{obs}/cm^{-1}	σ	N	Δ	E_{obs}/cm^{-1}	σ	N	Δ	E_{obs}/cm^{-1}	σ	N	Δ
12 2 10	11 921.4033	0.6	2	−1	−29	13 277.4641		1	−37								
12 3 10	11 927.3058	1.1	2	7	−28												
12 3 9	12 001.6749	1.6	2	−1	−30												
12 4 9	12 034.8363	1.9	2	8	−28												
12 4 8	12 063.8227		1	6	−29												
12 5 8	*12 145.2318	1.6	2	−37	−26												
12 5 7	*12 150.2251	4.4	2	−55	−27												
12 6 7	*12 273.3380		1	−34	−23												
13 0 13	11 832.7179	0.1	3	2	−29	13 164.0834		1	−34								
13 1 13	11 832.7179	0.0	2	−2	−29	13 164.3547		1	−36								
13 1 12	11 984.8520		1	10	−29	13 331.3642		1	−36								
13 2 12	11 985.0419	0.1	2	−1	−28												
13 2 11	12 113.5813		1	−1	−29												
13 3 11	12 116.9235		1	−11	−31												
13 3 10	12 209.0071	2.1	2	−2	−31												
13 4 10	12 232.7217		1	11	−29												
13 4 9	12 275.9915		1	11	−30												
14 0 14	12 010.5785		1	11	−31	13 340.6434		1	−37								
14 1 14	12 010.5545		1	−10	−29	13 340.6674		1	−37								
14 1 13	*12 174.6229		1	−528	−23												
14 2 13	12 175.2537	1.1	2	5	−28												
14 2 12	12 317.0492		1	−9	−30												
14 3 12	12 318.8821		1	−15	−32												
14 3 11	12 428.1375		1	−4	−30												
14 4 11	12 444.0427		1	6	−33												
14 4 10	12 503.9766		1	2	−33												
15 0 15	12 200.4484		1	−5	−31												
15 1 15	12 200.4602		1	6	−30												
15 1 14	*12 377.3476		1	−59	−29												
15 2 14	*12 377.4911		1	37	−29												
15 2 13	*12 531.9700		1	−23	−33												
15 3 13	12 532.9819		1	5	−31												
15 3 12	12 658.2709		1	−3	−32												
16 0 16	12 402.3362		1	−6	−32												
16 1 16	12 402.3310		1	−11	−32												
16 2 15	12 591.6144		1	3	−32												
17 0 17	12 616.1902		1	3	−32												
17 1 17	12 616.1931		1	6	−34												

[a] N is the number of lines used for the upper energy level determination and σ denotes the corresponding experimental uncertainty in 10^{-3} cm^{-1} units. Δ is the difference between the experimental energy level and the predictions of ref. 15 in 10^{-2} cm^{-1} units. For the (003) state, we also give the difference, δ, between the experimental and calculated (EH) energy level in 10^{-3} cm^{-1} units (* denotes energy level excluded from the EH fitting). A number of energy levels of the (112) state (marked by I) were first determined by ICLAS in ref. 13.

example of strong perturbation concerns the [918] (400) level at 11 064.2217 cm^{-1} coupled with a level at 11 067.8104 cm^{-1} (mis)assigned to the same rovibrational state by SP. Using the EH approach, we could assign this level, derived from three weak observed lines, to the [918] level of the highly excited pure bending state (080). The (400) state seems to be also perturbed by other dark states like (150) and (131), which makes accurate EH fitting problematical.

Rotational energy levels of the (032) and (112) states were derived in ref. 13 from hot transitions from the (010) state observed in the 9600–10 100 cm^{-1} spectral region. In the considered spectral region, weak transitions belonging mostly to the (112)–(000) band were assigned, and 43 extra levels could be determined. The (032) and (112) states are linked by a strong Fermi-type resonance interaction, leading to a nearly equal mixing of high K_a sublevels and thus to an ambiguity in the vibrational assignment. An rms of 0.022 cm^{-1} could be achieved for 84 energy levels (six levels excluded) with 18 varied parameters (not given), but the influence of other dark states on the (032)–(112) dyad hampered a satisfactory EH fitting.

The (013) state interacts mainly with the (330) and (141) dark states. As the vibrational energies of the (013) and (330) states are close - 11 969.76 and 11 958.26 cm^{-1} respectively - the interaction is already important for small J and K_a values. This interaction induces relatively strong (up to 1.1×10^{-4} cm^{-2}atm^{-1}) transitions to the $K_a = 1$ rotational levels allowing for the retrieval of nine experimental energy levels for the (330) state. We have already stressed the overall good agreement between the SP calculated and experimental intensities, but in the specific case of the (013)–(330) interaction, the calculated intensities of both the (330)–(000) transitions and the corresponding resonance-partners of the (013)–(000) band seem to be strongly distorted. For example, the calculated intensities are 2.5–3 times underestimated for transitions to the [313] (330) upper level, while those for transitions sharing the [312] (330) level seem to be overestimated by a factor of 2.

The resonance interaction between the $K_a = 4$ energy levels of the (013) state and those of the (141) state at 11 804.57 cm^{-1} is very strong. Seven energy levels of the (141) state were derived through transitions borrowing their intensities from

Table 3 Rotational energy levels (cm^{-1}) of the vibrational states of HDO derived in the 10 110–12 215 cm^{-1} spectral region[a]

$J\ K_aK_c$	E_{obs}/cm^{-1}	σ	N	Δ	$J\ K_aK_c$	E_{obs}/cm^{-1}	σ	N	Δ	$J\ K_aK_c$	E_{obs}/cm^{-1}	σ	N	Δ
	(032)					(051)					(141)			
0 0 0	11 242.923 I		1	−14	2 2 1	10 476.2865		1	4	4 4 1	12 344.8847		1	−14
1 0 1	11 258.346 I	3	2	−13	2 2 0	10 476.5950	5.0	2	4	4 4 0	12 344.8828		1	−15
1 1 1	11 276.3265 F		1	−13	3 2 2	10 521.9172		1	11	5 4 1	12 423.1458		1	−16
1 1 0	11 279.734 I		1	−15	3 2 1	10 523.4100	1.1	3	11	6 3 3	12 340.9520		1	−14
2 0 2	11 288.739 I	1	2	−14	4 2 3	10 590.5170		1	0	6 4 3	12 516.8737		1	−15
2 1 2	11 303.737 I		1	−14	4 2 2	10 594.5649	1.0	2	−2	6 4 2	12 517.1675		1	−17
2 1 1	11 313.9513 IF		1	−15	5 1 4	10 620.4112	0.6	2	14	7 4 3	12 627.0978	6.2	2	−23
2 2 0	11 367.001 I	4	2	−14	5 2 4	10 665.9336	0.8	2	−6		(061)			
3 0 3	11 333.250 I	2	2	−15	5 2 3	10 675.1175		1	−6	5 4 2	12 330.0703	2.3	3	0
3 1 3	11 344.603 I	2	3	−14	6 1 5	10 724.4236		1	7		(080)			
3 1 2	11 364.961 I		1	−14	7 1 6	10 837.5803		1	6	6 2 4	10 929.6690	0.6	2	1
3 2 2	11 412.640 I	4	2	−14	7 3 5	11 019.2934	4.5	2	−2	9 1 8	11 067.8104	2.5	3	−9
3 2 1	11 415.0418 IF	1	2	−15		(320)					(211)			
3 3 1	11 503.428 I		1	−15	2 1 2	10 682.2028		1	27	0 0 0	10 403.1422		1	−7
4 0 4	11 390.832 I	2	2	−15	2 1 1	10 692.3246		1	27	1 0 1	10 417.9828	5.1	3	−6
4 1 4	11 398.624 I		1	−15	3 1 3	10 721.8179		1	26	1 1 1	10 433.9840	1.4	2	−6
4 1 3	11 432.263 I		1	−14	3 1 2	10 741.9097	0.3	2	28	1 1 0	10 436.8191		1	−5
4 2 2	11 479.879 I		1	−14	4 1 3	10 807.3968		1	28	2 0 2	10 447.3050	3.5	2	−5
5 1 5	11 465.5211 IF	1	2	−15	5 1 4	10 888.1707		1	27	2 1 2	10 460.8507		1	−6
5 1 4	11 515.150 I		1	−15	6 1 5	10 983.4895		1	26	2 1 1	10 469.3741	1.2	2	−5
5 2 4	11 549.348 I		1	−15	7 1 6	11 092.5192	1.9	5	43	2 2 1	10 516.7938		1	−7
5 2 3	11 562.525 I		1	−13	8 1 7	11 214.0069		1	23	3 0 3	10 490.4529	0.1	2	−5
5 3 3	11 642.629 I		1	−3		(330)				3 3 1	10 634.6125		1	−8
6 0 6	11 542.105 I	2	2	−14	2 1 2	12 026.5502		1	18	4 0 4	10 546.6118	0.7	2	−5
6 1 6	11 545.028 I	1	2	−14	2 1 1	12 036.3374		1	22	4 1 4	10 554.0936	0.1	2	−5
6 1 5	11 612.735 I		1	−13	3 1 3	12 065.6916	0.1	2	12	4 1 3	10 582.7202	3.1	2	−1
6 2 5	11 639.292 I	9	2	−15	3 1 2	12 085.6479	0.8	2	10	5 0 5	10 615.0610	0.8	2	−5
6 2 4	11 662.743 I		1	−16	4 1 4	12 118.2064	6.5	2	22	5 1 5	10 620.0143	1.9	2	−6
6 3 4	11 735.026 I		1	5	4 1 3	12 150.3998	0.6	2	16	6 0 6	10 695.4058		1	−6
7 0 7	11 635.213 I	3	2	−15	5 1 4	12 231.0306	2.7	2	21	6 1 6	10 698.5367	0.5	2	−3
7 1 7	11 636.891 I		1	−16	6 1 5	12 326.2977		1	21	7 0 7	10 787.5587		1	−5
7 2 6	11 743.065 I		1	−14	7 1 6	12 435.5690	1.5	2	13	7 1 7	10 789.4442		1	−5
7 2 5	11 780.050 I	9	2	−13		(102)					(131)			
8 0 8	11 740.001 I		1	−17	8 7 2	11 137.7422		1	−6	3 3 0	10 772.7864	4.2	2	−11
8 1 8	11 740.997 I	5	2	−14	8 7 1	11 137.7422		1	−6	4 3 1	10 835.2885	1.9	6	−11
9 0 9	11 856.590 I	5	2	−15	8 8 1	11 326.6453		1	−3					
9 1 9	11 857.248 I		1	−11	8 8 0	11 326.6453		1	−3					
	(022)													
11 5 6	11 399.1247		1	−8										

[a] N is the number of lines used for the upper energy level determination and σ denotes the corresponding experimental uncertainty in 10^{-3} cm^{-1}. Δ is the difference between the experimental energy level and the prediction of ref. 15 in 10^{-2} cm^{-1} units. For the (032) state only, we merge the levels presently determined from FT data (marked with *F*) with those obtained by ICLAS-VeCSEL[13] (marked with *I*). Note in particular that many levels of the (022)–(102) dyad were determined in ref. 13 but are not listed here.

the (013)–(000) lines. Though the (013) energy levels with $K_a = 3$ are very close to those of the (061) state with $K_a = 4$, perturbations were not evident, neither for line positions nor for intensities of the (013)–(000) transitions. However, the resonance link between the [532] (013) level at 12 330.1801 cm^{-1} and the [542] (061) level at 12 330.0703 cm^{-1} induces a remarkable intensity transfer to weak transitions of the (061)–(000) band. The [524] (061) energy level was observed through three strong lines (see Table 5) while SP intensities were calculated more than 10 times weaker than observed. This is the only case where we found such a significant failure in SP intensity calculations for HDO. The resonance interactions of the (013) state with the (330) and (141) states are strongly dominant: we could indeed reproduce 133 energy levels of the (013)–(330)–(141) triad within 0.021 cm^{-1} by varying 26 parameters and excluding six levels. Ideally, other interactions with dark states should be taken into account to approach the experimental accuracy of the energy levels.

We have gathered in Table 6 the high-order resonance interactions in HDO which were evident in our work, together with those previously reported. This table shows that these interactions couple mostly vibrational states with a large difference in the bending quantum number v_2. This characteristic interaction is the result of a strong centrifugal distortion effect in HDO, which is induced by a high amplitude bending motion near the linear configuration. Similar effects were discussed in detail for the main isotopomer H_2O.[24]

V. Conclusion

Experimental and theoretical study of the HDO *FT* absorption spectrum in the wide spectral region 10 110–12 215 cm^{-1} resulted in the derivation and assignment of a large dataset of rovibrational energy levels. The HDO synthetic spectrum of Schwenke and Partridge[15,16] appeared to be accurate enough to provide an overall complete spectral assignment. Calculations using the effective Hamiltonian approach performed in parallel helped us to understand the nature of resonance interactions in HDO and to confirm most SP assignments. The analyzed rovibrational energy levels of HDO were found to undergo strong resonance interactions inducing

Table 4 Rotational and centrifugal distortion constants of the (003) vibrational state of HDO (in cm^{-1}) and a comparison with previous studies[a]

	This work	Ref. 14	Ref. 17
E_v	10 631.68900(200)	10 631.6366(83)	10 631.681(4)
A	20.381736(320)	20.3814(21)	20.370(4)
B	9.069274(140)	9.06731(89)	9.093(2)
C	6.1700468(990)	6.17030(22)	6.149(1)
Δ_k	$9.5005(150) \times 10^{-3}$	$9.31(11) \times 10^{-3}$	$2.1(9) \times 10^{-3}$
Δ_{jk}	$5.4727(610) \times 10^{-4}$	$6.44(65) \times 10^{-4}$	$-34(2) \times 10^{-4}$
Δ_j	$3.96914(710) \times 10^{-4}$	$3.599(82) \times 10^{-4}$	$9.9(6) \times 10^{-4}$
δ_k	$1.7254(100) \times 10^{-3}$	$1.507(42) \times 10^{-3}$	$1.1(8) \times 10^{-3}$
δ_j	$1.40648(490) \times 10^{-4}$	$1.239(41) \times 10^{-4}$	$2.7(2) \times 10^{-4}$
H_k	$3.1672(260) \times 10^{-5}$	$3.39(19) \times 10^{-5}$	
H_{kj}	$-1.0015(150) \times 10^{-5}$	$-1.40(13) \times 10^{-5}$	
H_{jk}	$2.2330(540) \times 10^{-6}$	2.4×10^{-6}	
H_j	$4.044(170) \times 10^{-8}$	3.9×10^{-8}	
h_k	$1.4365(500) \times 10^{-5}$	1.8×10^{-5}	
h_{kj}	$9.583(450) \times 10^{-7}$	10.0×10^{-7}	
h_j	$1.863(120) \times 10^{-8}$	2.1×10^{-8}	

[a] Values in parentheses are the 1σ statistical error intervals.

Table 5 Comparison of the observed and calculated[16] line intensities of transitions to the (061) [542] upper state

$J\ K_a\ K_c$		Observed wavenumber/ cm^{-1}	Intensity/cm^{-2} atm^{-1}		Upper level/ cm^{-1}
Upper	Lower		SP[15,16]	Observed	
5 4 2	6 3 3	11 860.4100	1.4×10^{-6}	3.2×10^{-5}	12 330.0735
5 4 2	5 3 3	11 956.4026	1.6×10^{-6}	2.0×10^{-5}	12 330.0684
5 4 2	4 3 1	12 034.3914	1.9×10^{-6}	2.8×10^{-5}	12 330.0689

Table 6 Summary of the high-order resonance couplings evident in HDO

Resonance partner of $v_1v_2v_3$	Interacting states $v_1v_2v_3$–$v'_1v'_2v'_3$	Ref.
$v_1 \mp 4\ v_2\ v_3 \pm 3$	(411)–(014)	8
$v_1 \mp 3\ v_2 \pm 1\ v_3 \pm 2$	(302)–(014)	8
$v_1 \pm 3\ v_2 \pm 2\ v_3 \mp 3$	(003)–(320)	This work
	(013)–(330)	This work
$v_1 \pm 5\ v_2 \mp 2\ v_3 \mp 3$	(024)–(501)	11
$v_1 \pm 1\ v_2 \pm 3\ v_3 \mp 2$	(014)–(142)	8
	(023)–(151)	9
	(003)–(131)	This work
	(013)–(141)	This work
$v_1 \mp 2\ v_2 \pm 4\ v_3$	(200)–(040)	25
	(210)–(050)	26,27
$v_1 \mp 4\ v_2 \pm 5\ v_1 \pm 1$	(400)–(051)	This work
$v_1\ v_2 \pm 5\ v_3 \mp 2$	(004)–(052)	7
	(015)–(063)	11
	(013)–(061)	This work
	(003)–(051)	This work
	(014)–(062)	8
$v_1 \pm 2\ v_2 \pm 6\ v_3 \mp 4$	(015)–(271)	11
$v_1 \mp 3\ v_2 \pm 6\ v_3$	(300)–(060)	28
$v_1\ v_2 \pm 6\ v_3 \mp 2$	(022)–(080)	13
$v_1 \mp 1\ v_2 \pm 8\ v_3 \mp 2$	(142)–(0 12 0)	8
$v_1\ v_2 \pm 8\ v_3 \mp 3$	(003)–(080)	This work
$v_1 \pm 1\ v_2 \pm 9\ v_3 \mp 4$	(024)–(1 11 0)	11

considerable intensity redistribution between line-resonance partners. High-order resonance interactions coupling the (v_1, v_2, v_3) bright state to the $(v_1 \pm 1, v_2 \pm 3, v_3 \mp 2)$ and $(v_1, v_2 \pm 5, v_3 \mp 2)$ dark states were frequently observed in HDO both in the present analysis and in previous investigations.

The analysis of the observed spectrum illustrated the limits of both theoretical approaches used. The effective Hamiltonian approach could not be applied in the case of large sets of interacting states in particular when the experimental energy levels were unknown for most of the coupled states. On the other hand, SP calculations failed to reproduce properly the intensities of some strongly perturbed transitions. We hope that the results obtained in this paper will help for further development of theoretical models.

Acknowledgements

O. N. wishes to thank the University Joseph Fourier of Grenoble for the visiting Professorship, during which this work was carried out. This work is jointly supported by the National Natural Science Foundation of China (20103007), a collaborative project between CNRS and RFBR (PICS grant 01-05-22002), and between CNRS and the Chinese Academy of Science (N° 12491). O. N. acknowledges the financial support from the Russian Foundation for Basic Researches (grants N° 02-03-32512 and N° 02-07-90139). This work was partly supported by CNRS in the frame of the "Programme National de Chimie Atmosphérique" and the INTAS foundation (project 03-51-3394).

References

1 R. A. Toth, *J. Mol. Spectrosc.*, 1997, **186**, 66–89.
2 R. A. Toth, *J. Mol. Spectrosc.*, 1997, **186**, 276–292.
3 R. A. Toth, *J. Mol. Spectrosc.*, 1999, **195**, 73–97.
4 A. Jenouvrier, M. F. Merienne, M. Carleer, R. Colin, A.-C. Vandaele, P. F. Bernath, O. L. Polyansky and J. Tennyson, *J. Mol. Spectrosc.*, 2001, **209**, 165–168.
5 X. Wang, S. He, S. Hu, J. Zheng and Q. Zhu, *Chin. Phys.*, 2000, **09**, 885–891.
6 S. Hu, S. He, J. Zheng, X. Wang, Y. Ding and Q. Zhu, *Chin. Phys.*, 2001, **10**, 1021–1027.
7 O. Naumenko, E. Bertseva and A. Campargue, *J. Mol. Spectrosc.*, 1999, **197**, 122–132.
8 O. Naumenko and A. Campargue, *J. Mol. Spectrosc.*, 2000, **199**, 59–72.
9 O. Naumenko, E. Bertseva, A. Campargue and D. Schwenke, *J. Mol. Spectrosc.*, 2000, **201**, 297–309.
10 E. Bertseva, O. Naumenko and A. Campargue, *J. Mol. Spectrosc.*, 2000, **203**, 28–36.
11 A. Campargue, E. Bertseva and O. Naumenko, *J. Mol. Spectrosc.*, 2000, **204**, 94–105.
12 S. Hu, H. Lin, S. He, J. Cheng and Q. Zhu, *Phys. Chem. Chem. Phys.*, 1999, **1**, 3727–3730.
13 E. Bertseva, O. Naumenko and A. Campargue, *J. Mol. Spectrosc.*, 2003, **221**, 38–46.
14 A. D. Bykov, V. A. Kapitanov, O. V. Naumenko, T. M. Petrova, V. I. Serdyukov and L. Sinitsa, *J. Mol. Spectrosc.*, 1992, **153**, 197–207.
15 H. Partridge and D. W. Schwenke, *J. Chem. Phys.*, 1997, **106**, 4618–4639.
16 D. W. Schwenke and H. Partridge, *J. Chem. Phys.*, 2000, **113**, 6592–6597.
17 O. Votava, J. R. Fair, D. F. Plusquellic, E. Riedle and D. J. Nesbitt, *J. Chem. Phys.*, 1997, **107**, 8854–8865.
18 J. R. Fair, O. Votava and D. J. Nesbitt, *J. Chem. Phys.*, 1998, **108**, 72–80.
19 A. Bykov, O. Naumenko, A. Pshenichnikov, L. Sinitsa and A. Shcherbakov, *Optics and Spectroscopy*, 2003, **94**, 528–537.
20 R. Toth, *J. Mol. Spectrosc.*, 1993, **162**, 20–40.
21 S. S. Voronina, *Atmos. Ocean. Opt.*, 2002, **15**, 727–729.

22 O. L. Polyansky, *J. Mol. Spectrosc.*, 1985, **112**, 79–87.
23 J.-M. Flaud, C. Camy-Peyret, A. Bykov, O. Naumenko, T. Petrova, A. Scherbakov and L. N. Sinitsa, *J. Mol. Spectrosc.*, 1997, **183**, 300–309.
24 A. D. Bykov, O. V. Naumenko, L. N. Sinitsa, B. Voronin, J.-M. Flaud, C. Camy-Peyret and R. Lanquetin, *J. Mol. Spectrosc.*, 2001, **206**, 1–8.
25 A. D. Bykov, B. A. Voronin, O. V. Naumenko, L. N. Sinitsa and T. M. Petrova, *Atmos. Ocean. Opt.*, 1999, **12**, 786–791.
26 A. D. Bykov, O. V. Naumenko, L. N. Sinitsa, B. P. Winnewisser, M. Winnewisser, P. S. Ormsby and K. Narahari Rao, *SPIE*, 1993, **2205**, 248–252.
27 O. N. Ulenikov, S. Hu, E. S. Bekhtereva, G. A. Onopenko, X. Wang, S. He, J. Zheng and Q. Zhu, *J. Mol. Spectrosc.*, 2001, **208**, 224–235.
28 S. Hu, O. N. Ulenikov, G. A. Onopenko, E. S. Bekhtereva, S. He, X. Wang, H. Lin and Q. Zhu, *J. Mol. Spectrosc.*, 2000, **203**, 228–234.

